

# Towards Stable and Calibration-Free Motor Imagery BCIs via Graph-Based Transfer Learning

Rishan Patel<sup>1</sup>, Ziyue Zhu<sup>2</sup> Barney Bryson<sup>3</sup>, Tom Carlson<sup>2</sup> Dai Jiang<sup>1</sup>, and Andreas Demosthenous<sup>1</sup>

**Abstract**—Brain-computer interfaces (BCIs) based on electroencephalography (EEG) remain limited by signal nonstationarities across time and users, hindering real-world deployment. Traditional deep learning methods often require session-specific recalibration or rigid spatial priors, both of which are impractical in longitudinal or clinical settings. We propose a calibration-free, subject-independent framework that encodes EEG topologies using trial-wise Phase-Locking Value (PLV) connectivity and Graph Attention Networks (GAT). Evaluated under a Leave-One-Subject-Out (LOSO) protocol, our model significantly outperforms or matches seven baseline architectures, including domain-adaptive and convolutional pipelines. Results hold across two datasets involving both healthy participants and individuals with amyotrophic lateral sclerosis (ALS). Statistical analyses confirm performance robustness to moderate cognitive variability and inter-individual differences. These findings demonstrate that graph-based EEG representations can enable scalable, spontaneous BCI use, reducing the need for individualized retraining and advancing the feasibility of plug-and-play neurotechnologies.

**Index Terms**—Motor Imagery, Brain-Computer Interface, Transfer Learning, Graph Neural Networks

## I. INTRODUCTION

Electroencephalography (EEG)-based brain-computer interfaces (BCIs) have long held promise for restoring autonomy in patients with motor impairments, offering a non-invasive gateway to communication and control. Yet, despite decades of innovation, a core limitation persists: nonstationarity in neural signals over time. The disconnect between robust laboratory performance and practical, long-term usability remains particularly stark in clinical populations such as Amyotrophic Lateral Sclerosis (ALS), where progressive neurodegeneration and cortical reorganization profoundly alter the structure of EEG signals over weeks or months [1]. Despite this known issue, current research embodies major oversights in testing healthy participants in longitudinal settings who suffer from nonstationarity equally as ALS.

This evolving neural landscape degrades classifier accuracy, demanding repeated recalibration and limiting real-world deployment [2], [3]. Traditional motor imagery (MI) classifiers designed around contralateral motor features struggle to adapt to these slow, non-linear shifts. While some success has been found with adaptive models, they typically fall short of

capturing the full temporal and interpersonal variability present in EEG signals [4]–[8] during training and evaluation due to experimental design choices.

Broadly, two strategies have emerged to address nonstationarity. One increases data volume by collecting more trials or enriching trial complexity, often infeasible in clinical settings. The second adapts the model itself, typically through online learning or recalibration. However, both approaches implicitly assume the constancy of underlying signal generators or rely heavily on hand-crafted features. Yet, recent findings suggest that MI involves distributed, dynamic networks extending beyond the canonical sensorimotor strip [9], [10]. This calls for a shift in perspective from static, region-specific models to global approaches that account for the full functional topology of the brain.

Transfer learning is a strategy to address challenges associated with limited data and inter/intra-subject variability. By leveraging knowledge acquired from a pre-trained model on one dataset, transfer learning techniques enable the adaptation of these models to new, yet related tasks, thereby reducing calibration time and improving overall performance [11]. However, the literature shows transfer learning is not typically employed to specifically address longitudinal nonstationarities especially in graphical pipelines. While recent studies have demonstrated the effectiveness of domain adaptation and fine-tuning approaches in mitigating nonstationarity in the context of motor imagery, these techniques often focus on short-term adaptations rather than the gradual, longitudinal shifts seen in clinical populations and real-world BCI use [12]–[15]. Moreover, the integration of transfer learning with advanced architectures, such as graph-based models has not yet been properly explored [16], [17]. This line of research enhances model generalizability, expanding a relatively new line of enquiry into Graph Neural Networks (GNNs), paving the way for more robust and user-friendly BCI systems.

Our prior work introduced a graphical connectivity framework that captures these topological dynamics using Phase-Locking Value (PLV) as a measure of functional synchrony across electrodes [18]. We observed that even as overall connectivity fluctuated between sessions, graph-based representations retained consistent hubs, suggesting stable, underlying network structures. These findings support emerging evidence that GNNs can learn subject-general features robust to session drift and inter-subject variability [19].

In this study, we extend that hypothesis and propose a subject-independent framework for classifying left- and right-hand motor imagery. Rather than suppress variability, we leverage it, while anchoring our models on the shared, sta-

<sup>1</sup>Rishan Patel, Dai Jiang and Andreas Demosthenous are with the Dept. of Electrical and Electronic Engineering, University College London, London, WC1E 7HB, UK (e-mail: uceerjp@ucl.ac.uk, d.jiang@ucl.ac.uk, a.demosthenous@ucl.ac.uk).

<sup>2</sup>Ziyue Zhu and Tom Carlson are with the Aspire Create, University College London, Royal National Orthopaedic Hospital, Stanmore, HA7 4LP, UK (e-mail: t.carlson@ucl.ac.uk).

<sup>3</sup>Barney Bryson is with the Institute of Neurology, University College London, London, WC1E 7HB, UK (e-mail: b.bryson@ucl.ac.uk).

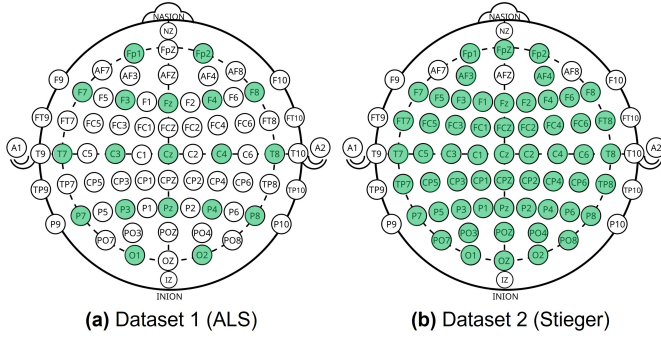


Fig. 1: Electrode configurations for (a) ALS and (b) Stieger Dataset

ble connectivity patterns that persist across individuals. By computing trial-wise PLV graphs and training a Graph Attention Network (GAT) using Leave-One-Subject-Out-Cross-Validation (LOSOCV) evaluation, we demonstrate that robust performance is achievable even for unseen participants compared to state-of-the-art (SOTA), including ALS patients over multiple, nonstationary recordings. This approach has the potential to reduce calibration burden and improve reliability in real-world BCI systems bringing us one step closer to truly adaptive, and functional neurotechnology.

## II. METHODOLOGY

### A. Datasets

Our hypothesis stems from observed clustering patterns during a controlled left–right cursor control task in [20], which produces distinct graph-based representations of brain activity. This protocol provides high experimental control and reproducibility, distinguishing it from less structured paradigms found in smaller longitudinal datasets such as [21]. We propose that our method is best suited to datasets with protocol homogeneity, particularly those engaging similar cortical processing hubs, like cursor control. In contrast, datasets lacking clear task instructions or feedback mechanisms often fail to elicit consistent neural patterns across subjects, limiting the generalizability of our framework. To ensure fair evaluation, we selected two datasets featuring longitudinal, homogeneous tasks with enough methodological variation to demonstrate effectiveness. Thereby offering high translational value for real-world ALS control applications.

1) *Dataset 1 (ALS)* [20]: Eight ALS patients (45.5–74 years; ALSFRS-R: 0–46; TSSO: 12–113 months) participated in four sessions of left–right cursor control over 1–2 months. EEG was recorded from nineteen channels (10–20 system; linked earlobes reference; FPz ground) using the g.USBamp system and BCI2000, with impedances kept below 10 k $\Omega$ . Each participant completed approximately 150–160 trials of left-/right-hand MI, beginning with a calibration run followed by online feedback sessions.

2) *Dataset 2 (Stieger)* [22]: Sixty-two participants (mindfulness: 33; control: 29) completed an experiment following an 8-week Mindfulness-Based Stress Reduction training (MSBR)

across 6–10 BCI sessions. EEG was recorded from 64 channels (10–10 system) at 250 Hz with a 1–100 Hz bandpass filter. Each session included 18 runs (6 each for left/right, up/down, and 2D cursor control), with approximately 25 trials per run ( $\sim 3$  minutes). Cursor motion was based on mu band (8–12 Hz) power asymmetries: lateral motion by C3/C4 differences, vertical motion by imagery versus rest contrast. For this study, we used the first twenty participants (19–62 years; 6M/14F; 8 MBSR /12 Control), their first four sessions, and only the left/right MI trials (approximately 800–900 trials per participant).

### B. Feasibility of Graph-based Transfer Learning

To validate our hypothesis for the existence of subject-invariant features using graph-based methods, we compute the PLV between pairs of EEG electrodes for each subject. For each trial, the instantaneous phases of the EEG signals are extracted via the Hilbert transform, and the PLV between each unique electrode pair is computed as

$$\text{PLV} = \left| \frac{1}{T} \sum_{t=1}^T e^{i(\phi_2(t) - \phi_1(t))} \right| \quad (1)$$

where  $T$  is the number of time points and  $\phi_1(t)$  and  $\phi_2(t)$  are the instantaneous phases of the two signals. Per trial, this yields a square matrix ( $n \times n$ ), which can be represented as a time series tensor ( $n \times n \times t$ ) to capture nonstationarity in graphical form. To assess the invariance of the PLV time series for each electrode pair, we calculate the coefficient of variation (CV) across trials

$$\text{Coefficient of Variation} = \frac{\sigma}{\mu} \quad (2)$$

where  $\sigma$  is the standard deviation and  $\mu$  is the mean of each electrode pair time series. A low CV indicates that the PLV is stable over trials. Stability metrics are then aggregated across subjects. For each class, the mean CV matrix was computed by averaging the CV values from all subjects. Electrode pairs with the lowest mean CV were identified as the most stable and, thus, as potential subject-invariant features.

### C. Evaluation Protocol

In this study, we aim to classify MI tasks by pooling subjects to generalize for a new participant. This is achieved using the LOSOCV approach. Our methodology includes data preprocessing, graph construction, model training, and evaluation. Figure 2 provides a high-level overview of this pipeline.

1) *LOSOCV*: Testing our model in a LOSOCV approach by designating each participant as the test subject in turn. For a given test subject, the remaining participants constituted the training set. This split ensures the model is evaluated on unseen subjects, making the protocol highly relevant for real-world applications where calibration data from a new user may be scarce. There is no calibration data used in our method from the target subject.

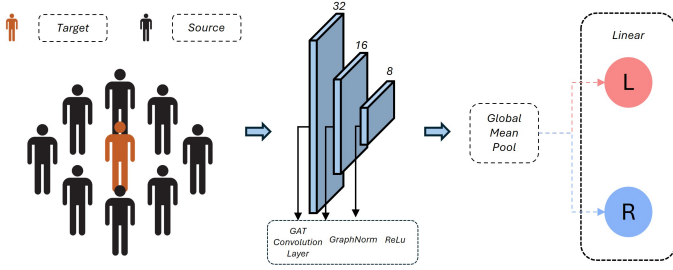


Fig. 2: High-level architecture of our proposed LOSOCV protocol. A subset of participants (source) is used to train the GAT model, while one participant (target) remains unseen during training.

Layer	Configuration
Layer 1	GATv2Conv(in = Input Chans, out=32, heads=8, concat=True)
Layer 2	GATv2Conv(in=32 $\times$ 8, out=16, heads=8, concat=True)
Layer 3	GATv2Conv(in=16 $\times$ 8, out=8, heads=8, concat=False)
Pooling	Global mean pooling
Classifier	Linear(8 $\rightarrow$ 2)

TABLE I: Overview of the GAT-based Architecture.

2) *Model Architecture and Training*: Our model (rPLV-GAT) comprising three GATv2Conv layers, is demonstrated by Fig. 2 and Table I. Hyperparameters (learning rate, batch size) were selected based on standard practice for EEG decoding, and no extensive tuning was performed to maintain fairness across models. We use the Adam optimizer (learning rate = 0.001) and cross-entropy loss for 25 epochs with a batch size of 32. All results for Dataset 1 were compiled on a Intel Core vPro i7 32GB PC and Dataset 2 on a NVidia V100 32GB GPU due to its significantly larger size.

3) *Benchmark Models*: To benchmark our models against the SOTA, we compare performance with seven publicly available approaches: LMDANet [23], a channel- and depth-wise attention network; FTL [24], a federated transfer learning network requiring 20% calibration from unseen subjects; a 1D CNN by Mattioli et al. [25]; MIN2Net, a calibration-free subject-independent model by Autthasan et al.; and three additional baselines: GCNsNet (with Pearsons Correlation Coefficient for accurate replication and our PLV method) [26], EEGNet [27], and ShallowConvNet [28]. All code is available on Github to reproduce all models<sup>1</sup>.

### III. RESULTS

Three of the benchmark models (ShallowConvNet, LMDA, and MIN2NET) could not be executed on Dataset 2 due to prohibitive computational requirements, despite attempts to optimize memory usage and adapt source libraries to our available GPU architecture. Notably, LMDA and MIN2NET were incompatible with NVIDIA Volta-class GPUs, which were the only high-memory devices accessible for this study.

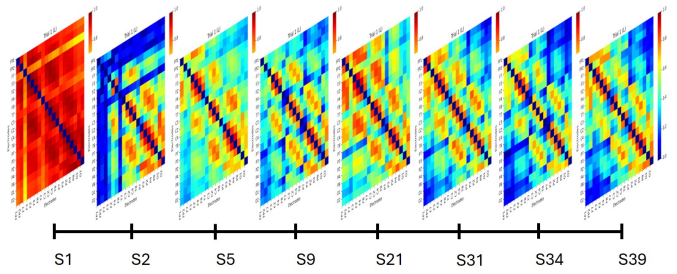


Fig. 3: PLV connectivity matrices for Left MI (Trial 1, Session 1) across subjects from Dataset 1. Despite inter and intra-subject variability in overall signal strength and classification performance, consistent connectivity patterns and prominent functional hubs emerge across participants, particularly along sensorimotor regions. These recurring structures suggest shared underlying neurophysiological mechanisms in cursor MI tasks and support the viability of cross-subject graph-based feature extraction.

In contrast, our graph-based preprocessing reduced raw time-series data ( $\sim 70$ GB) to approximately 30 GB of connectivity matrices, significantly improving memory efficiency. These challenges highlight a critical limitation: models with high memory footprints or restricted hardware compatibility may be unsuitable for large-scale, real-time, or wearable BCI applications. This underscores the practical advantage of lightweight, topologically structured approaches such as rPLV-GAT, which offer scalability without sacrificing performance.

We demonstrate the connectivity matrices of each first trial per participant for Dataset 1 in Fig. 3. It is evident that there exists constant hubs shared between participants, therefore encouraging our usage of Graph inputs. Quantitatively, this can be compressed into a square matrix as shown in Fig. 4b, where the time-invariance can be established for a participant, per electrode-pairs. Finally, we find that these time-invariant features persist across all participants when taking the mean CV matrices as seen in Fig. 5, thereby validating our hypothesis that PLV matrices are suitable for subject-independent MI classification tasks.

Across both datasets, our GAT-based framework demonstrated competitive or superior performance compared to seven baseline models, as seen in Fig. 6. In Dataset 1 (ALS cohort), our model achieved a mean accuracy of 62.65% across participants, outperforming all baselines. In Dataset 2 (healthy cohort), we show comparatively high generalization ability at 59.21%, despite greater inter-subject variability. Individual participant scatter further highlights model consistency across subjects, underscoring the viability of leveraging graph-based EEG representations for calibration-free MI decoding.

Statistical comparisons using the Wilcoxon signed-rank test revealed that rPLVGAT significantly outperformed five of seven baselines in Dataset 1, including LMDA ( $p = 0.0078$ ), FTL ( $p = 0.0391$ ), 1D CNN ( $p = 0.0078$ ), MIN2NET ( $p = 0.0156$ ), and GCNs-Net ( $p = 0.0469$ ). While ShallowConvNet

<sup>1</sup><https://github.com/rishannp/Subject-Independent-Graphical-Models>

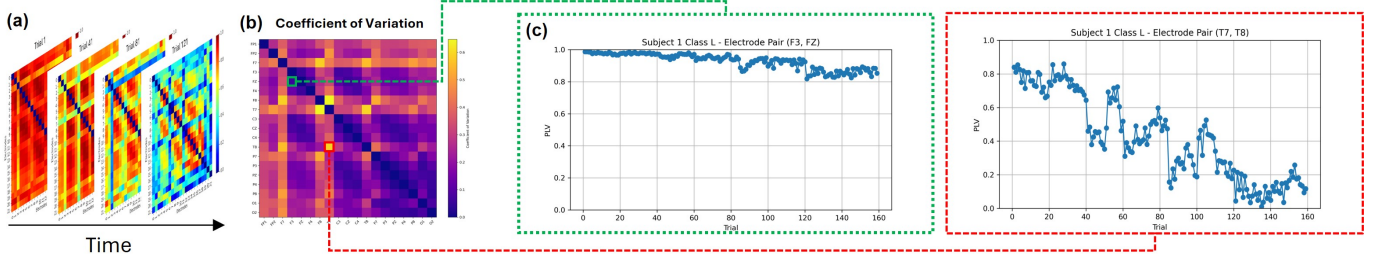


Fig. 4: **(a)** PLV matrices for the first trial in each session for Subject 1 (Dataset 1), illustrating the temporal evolution of functional connectivity over the course of data collection. A gradual reduction in global synchrony is observed, reflecting potential neurophysiological changes across sessions. **(b)** CV matrix for Subject 1’s Left MI class, computed across all trials, highlighting regions of high inter-trial variability in connectivity (e.g., T7–T8) versus stable electrode pairs (e.g., F3–Fz). **(c)** PLV trajectories over time for two exemplar electrode pairs: one stable (F3–Fz, green box) and one highly variable (T7–T8, red box), demonstrating differential reliability of connectivity patterns within the same subject and condition.

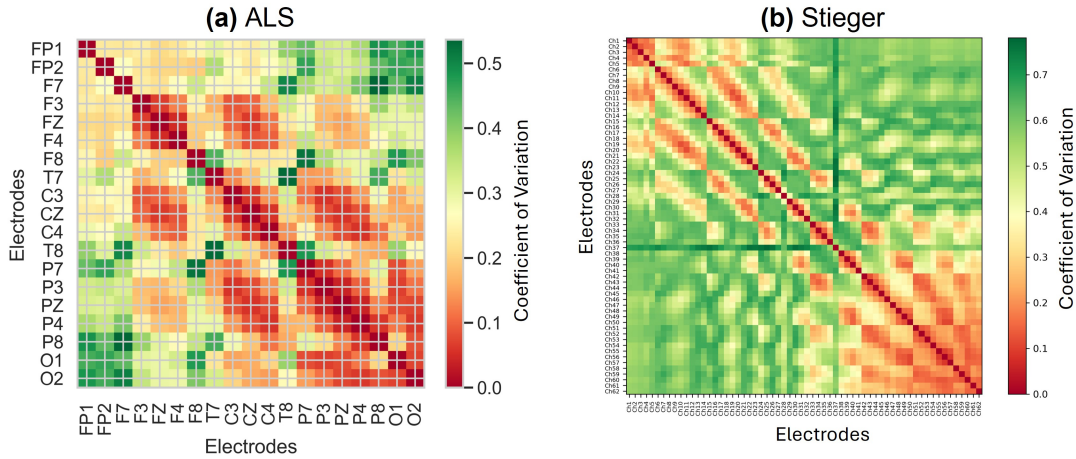


Fig. 5: Mean CV matrices across all subjects for: **(a)** Dataset 1 and **(b)** Dataset 2. These matrices highlight the consistency of connectivity across trials, with warmer colours (red) indicating stable electrode pair connections and cooler colours (green) indicating higher variability. Notably, both datasets exhibit preserved stable hubs, particularly in frontal and central regions suggesting shared underlying connectivity features across populations despite differences in health status and recording setups.

was marginal ( $p = 0.0547$ ), EEGNet showed no significant difference ( $p = 0.4609$ ). In Dataset 2, rPLVGAT showed highly significant improvements over EEGNet ( $p < 0.0001$ ), FTL ( $p = 0.0001$ ), and 1D CNN ( $p < 0.0001$ ), while GCNs-Net exhibited comparable performance ( $p = 0.1978$ ). These results reinforce the model’s robustness and statistical reliability across both ALS and healthy populations.

In these results, we have reported GCNs-Net with PLV connectivity rather than Pearson correlation, as the performance was significantly improved compared to the original implementation [18], [26].

#### IV. DISCUSSION

This study contributes to the advancement of calibration-free MI decoding with a focus on both cross-subject and longitudinal generalization: key requirements for real-world BCI deployment. Our findings indicate that, despite expected variability in EEG signals and decoding performance, stable functional connectivity patterns persist across participants,

particularly within fronto-central and parietal-occipital regions (Figs. 3–5). These patterns corroborate emerging evidence that MI engages distributed, rather than purely contralateral, cortical networks [9], [10]. By leveraging phase-locking value connectivity, our model identifies consistent graph structures, even in the face of nonstationarity across sessions and individuals. The CV offered an interpretable metric of feature stability (Fig. 4), revealing both stable and dynamic hubs across cohorts. These subject-invariant structures enable a viable basis for transfer learning within cohorts (Fig. 5), a capability not readily captured by conventional architectures such as EEGNet that operate on raw time-series inputs.

Evaluated under a LOSOCV scheme, our rPLV-GAT model demonstrated competitive or superior performance against seven benchmark models (Fig. 6). Importantly, this was achieved without requiring any calibration data from the target subject. A Mann–Whitney U test revealed no significant performance difference between mindfulness-trained and control



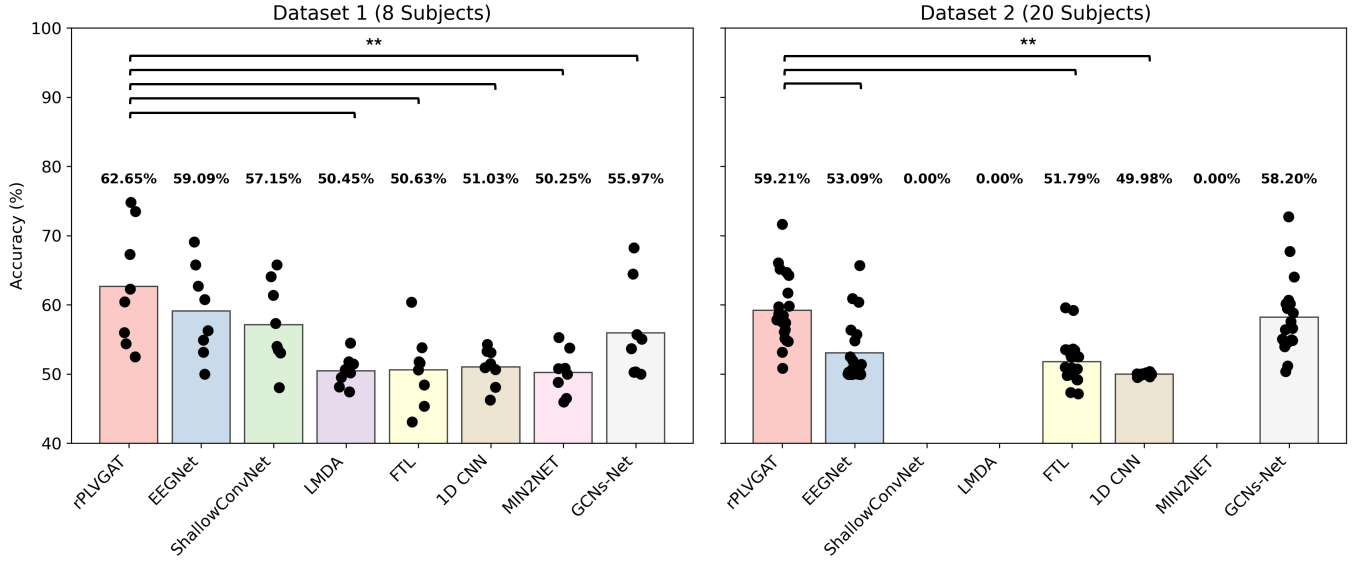


Fig. 6: Subject and Model-wise performance over Dataset 1 and 2. Asterisks (\*\*) denote models for which rPLVGAT significantly outperformed baselines using the Wilcoxon signed-rank test ( $p < 0.05$ )

participants in Dataset 2 ( $p=0.9101$ ), further reinforcing the model’s robustness to moderate cognitive variability. These results validate the capacity of graph-based models to encode topological EEG dynamics that persist across substantial inter-individual and temporal variation.

Beyond eliminating offline calibration, the broader appeal of calibration-free decoding lies in its operational flexibility. In practical scenarios, such as assistive communication or mobility control, users must often engage BCIs spontaneously. Calibration procedures introduce latency, cognitive fatigue, and session-to-session variability, all of which undermine usability. A model that generalizes across users and sessions, therefore, enables immediate, low-friction engagement and supports opportunistic usage patterns critical for long-term adoption.

Clinically, this capability is particularly relevant for populations such as individuals with ALS, who may lack the physical or cognitive resources to participate in frequent recalibration sessions. Our model offers a promising framework for adaptive decoding, one that could, in future iterations, fine-tune only on the most stable features while discarding less reliable ones. Compared to alternatives like GCNsNet, which rely on static Pearson correlation graphs, our use of PLV yielded demonstrable improvements in both signal stability and classification performance [18] catapulting the accuracy to second place for both datasets.

That said, calibration-based pipelines, especially those involving session-wise fine-tuning, can outperform subject-independent methods in certain individuals. However, they come at the cost of increased data collection, processing time, and user effort, which limits scalability and inclusivity. Moreover, such pipelines often yield disproportionate benefits for high-performing individuals, leaving users with low baseline

controllability underserved.

In contrast, real-world use cases increasingly incorporate context-aware shared control, where decoding accuracy thresholds are relaxed in favour of user-centric system design [29]. Our model, achieving comparable or higher accuracy without calibration, is thus well-positioned for integration into such hybrid BCI systems.

Looking ahead, a promising future direction lies in lightweight online adaptation. Calibration-free models could serve as initialization frameworks, with subsequent online refinement guided by consistency regularization, or self-supervised proxy tasks. Such strategies would minimize user burden while enabling gradual personalization, merging the advantages of calibration-free and adaptive learning pipelines.

Nevertheless, several limitations warrant attention. First, while overall classification performance improved across the board, gains were not evenly distributed: low-performing individuals (50–55% accuracy) benefited less. Assuming similar engagement levels [18], this suggests a persistent gap in feature representation across subjects. Techniques such as Maximum Mean Discrepancy (MMD) alignment may help minimize this divergence. Although MMD-based benchmark models did not yield strong results in our tests, integrating them into graph-based pipelines remains a promising research avenue.

From a data perspective, our analysis on Dataset 2 used only a fraction of the available samples, approximately one-third of the participants and sessions (20 Participants out of 62, with only 4 sessions used out of 7-11). This dataset, due to its richness, high temporal density, and detailed metadata, represents a rare resource in MI research. We advocate for increased community focus on leveraging such datasets over smaller, less structured collections. Furthermore, as dataset

scale increases, so too should architectural capacity. While our model handled moderate-scale graphs effectively, future work should explore scaling GNN depth and expressivity to accommodate richer temporal structure and higher node counts.

Finally, this study focused exclusively on cursor-control MI tasks. Whether the subject-general graph structure we observed persists across other paradigms, such as imagined speech, attention modulation, or affective tasks remains to be seen.

## V. CONCLUSION

We proposed a subject-independent, graph-based framework for MI EEG classification, addressing the challenge of longitudinal nonstationarity. By leveraging stable connectivity patterns via PLV graphs and GAT-based models, we demonstrated competitive performance without requiring subject-specific calibration. Our results support the viability of topological EEG representations for scalable, user-friendly BCI systems. Future work will extend this framework to other paradigms and investigate adaptive strategies for further improving performance among low-performing individuals.

## ACKNOWLEDGMENT

This work was supported by the EPSRC Doctoral Training Programme (Grant EP/W524335/1). We thank Dr. Geronimo (Penn State University) for providing dataset access, and the authors of benchmark models for openly sharing their code.

## REFERENCES

- [1] K. Nihei, A. C. McKee, and N. W. Kowall, "Patterns of neuronal degeneration in the motor cortex of amyotrophic lateral sclerosis patients," *Acta neuropathologica*, vol. 86, pp. 55–64, 6 1993.
- [2] J. D. Bennett, S. E. John, D. B. Grayden, and A. N. Burkitt, "A neurophysiological approach to spatial filter selection for adaptive brain-computer interfaces," *Journal of Neural Engineering*, vol. 18, p. 026017, mar 2021.
- [3] T. Fomina, G. Lohmann, M. Erb, T. Ethofer, B. Schölkopf, and M. Grosse-Wentrup, "Self-regulation of brain rhythms in the precuneus: a novel bci paradigm for patients with als," *Journal of Neural Engineering*, vol. 13, p. 066021, nov 2016.
- [4] T. Lotey, P. Keserwani, G. Wasnik, and P. P. Roy, "Cross-session motor imagery eeg classification using self-supervised contrastive learning," in *2022 26th International Conference on Pattern Recognition (ICPR)*, pp. 975–981, 2022.
- [5] S. R. Liyanage, C. Guan, H. Zhang, K. K. Ang, J. Xu, and T. H. Lee, "Dynamically weighted ensemble classification for non-stationary eeg processing," *Journal of Neural Engineering*, vol. 10, p. 036007, apr 2013.
- [6] M. Arvaneh, C. Guan, K. K. Ang, and C. Quek, "Eeg data space adaptation to reduce intersession nonstationarity in brain-computer interface," *Neural Computation*, vol. 25, pp. 2146–2171, 08 2013.
- [7] S. Chua, Y. Tao, and R. Q. So, "Improved decoding of eeg-based motor imagery using convolutional neural network and data space adaptation," in *2019 IEEE EMBS International Conference on Biomedical Health Informatics (BHI)*, pp. 1–4, 2019.
- [8] B.-H. Lee, J.-H. Jeong, and S.-W. Lee, "Sessionnet: Feature similarity-based weighted ensemble learning for motor imagery classification," *IEEE Access*, vol. 8, pp. 134524–134535, 2020.
- [9] M. C. Ottenhoff, M. Verwoert, S. Goulis, S. Tousseyn, J. P. van Dijk, M. M. Shanechi, O. G. Sani, P. Kubben, and C. Herff, "Decoding continuous goal-directed movement from human brain-wide intracranial recordings," *bioRxiv*, 2025.
- [10] A. Dillen, F. Ghaffari, O. Romain, B. Vanderborght, R. Meeusen, B. Roelands, and K. De Pauw, "Optimal sensor set for decoding motor imagery from eeg," in *2023 11th International IEEE/EMBS Conference on Neural Engineering (NER)*, pp. 1–4, 2023.
- [11] R. Liu, S. Kumar, H. Alawieh, E. Carnahan, and J. del R. Millán, "On transfer learning for naive brain computer interface users," in *2023 11th International IEEE/EMBS Conference on Neural Engineering (NER)*, pp. 1–5, 2023.
- [12] Y. Wang, J. Wang, W. Wang, J. Su, C. Buntergchit, and Z.-G. Hou, "Tfit: A task-free transfer learning strategy for eeg-based cross-subject and cross-dataset motor imagery bci," *IEEE Transactions on Biomedical Engineering*, vol. 72, no. 2, pp. 810–821, 2025.
- [13] H. Zhi, T. Yu, Z. Gu, Z. Lin, L. Che, Y. Li, and Z. Yu, "Supervised contrastive learning-based domain generalization network for cross-subject motor decoding," *IEEE Transactions on Biomedical Engineering*, vol. 72, no. 1, pp. 401–412, 2025.
- [14] Q. She, T. Chen, F. Fang, J. Zhang, Y. Gao, and Y. Zhang, "Improved domain adaptation network based on wasserstein distance for motor imagery eeg classification," *IEEE Transactions on Neural Systems and Rehabilitation Engineering*, vol. 31, pp. 1137–1148, 2023.
- [15] J. Han, X. Gu, G.-Z. Yang, and B. Lo, "Noise-factorized disentangled representation learning for generalizable motor imagery eeg classification," *IEEE Journal of Biomedical and Health Informatics*, vol. 28, no. 2, pp. 765–776, 2024.
- [16] J. Zhang, K. Li, B. Yang, and Z. Zhao, "Cross-dataset motor imagery decoding — a transfer learning assisted graph convolutional network approach," *Biomedical Signal Processing and Control*, vol. 102, p. 107213, 2025.
- [17] J. Han, X. Wei, and A. A. Faisal, "Eeg decoding for datasets with heterogenous electrode configurations using transfer learning graph neural networks," *Journal of Neural Engineering*, vol. 20, p. 066027, dec 2023.
- [18] R. Patel, Z. Zhu, B. Bryson, T. Carlson, D. Jiang, and A. Demosthenous, "Advancing eeg classification for neurodegenerative conditions using bci: A graph attention approach with phase synchrony," *Neuroelectronics*, vol. 2, no. 1, 2025.
- [19] D. Klepl, M. Wu, and F. He, "Graph neural network-based eeg classification: A survey," *IEEE Transactions on Neural Systems and Rehabilitation Engineering*, vol. 32, pp. 493–503, 2024.
- [20] R. Patel, D. Jiang, B. Bryson, T. Carlson, A. Demosthenous, and A. Geronimo, "Longitudinal ALS EEG dataset for motor imagery studies," *FigShare*, jan 2025. DOI: <https://doi.org/10.5522/04/28156016.v110.5522/04/28156016.v1>.
- [21] J. Ma, B. Yang, W. Qiu, Y. Li, S. Gao, and X. Xia, "A large eeg dataset for studying cross-session variability in motor imagery brain-computer interface," *Scientific Data*, vol. 9, 12 2022.
- [22] J. Stieger, "Human eeg dataset for brain-computer interface and meditation," *FigShare*, Feb. 2021. DOI: <https://doi.org/10.6084/m9.figshare.13123148.v1>.
- [23] Z. Miao, M. Zhao, X. Zhang, and D. Ming, "Lmda-net: a lightweight multi-dimensional attention network for general eeg-based brain-computer interfaces and interpretability," *NeuroImage*, vol. 276, p. 120209, 2023.
- [24] C. Ju, D. Gao, R. Mane, B. Tan, Y. Liu, and C. Guan, "Federated transfer learning for eeg signal classification," in *2020 42nd Annual International Conference of the IEEE Engineering in Medicine Biology Society (EMBC)*, pp. 3040–3045, 2020.
- [25] F. Mattioli, C. Porcaro, and G. Baldassarre, "A 1d cnn for high accuracy classification and transfer learning in motor imagery eeg-based brain-computer interface," *Journal of Neural Engineering*, vol. 18, p. 066053, jan 2022.
- [26] Y. Hou, S. Jia, X. Lun, Z. Hao, Y. Shi, Y. Li, R. Zeng, and J. Lv, "Gens-net: A graph convolutional neural network approach for decoding time-resolved eeg motor imagery signals," *IEEE Transactions on Neural Networks and Learning Systems*, vol. 35, no. 6, pp. 7312–7323, 2024.
- [27] V. J. Lawhern, A. J. Solon, N. R. Waytowich, S. M. Gordon, C. P. Hung, and B. J. Lance, "Eegnet: a compact convolutional neural network for eeg-based brain-computer interfaces," *Journal of Neural Engineering*, vol. 15, p. 056013, 7 2018.
- [28] R. T. Schirmer, J. T. Springenberg, L. D. J. Fiederer, M. Glasstetter, K. Eggersperger, M. Tangermann, F. Hutter, W. Burgard, and T. Ball, "Deep learning with convolutional neural networks for eeg decoding and visualization," *Human brain mapping*, vol. 38, pp. 5391–5420, 11 2017.
- [29] B. Xu, D. Liu, M. Xue, M. Miao, C. Hu, and A. Song, "Continuous shared control of a mobile robot with brain-computer interface and autonomous navigation for daily assistance," *Computational and Structural Biotechnology Journal*, vol. 22, pp. 3–16, 2023.